Fusion reactions of ^{58,64}Ni + ^{124}Sn

C. L. Jiang,[1,*] A. M. Stefanini,[2] H. Esbensen,[1] K. E. Rehm,[1] S. Almaraz-Calderon,[1] M. L. Avila,[1] B. B. Back,[1] D. Bourgin,[3] L. Corradi,[2] S. Courtin,[3] E. Fioretto,[2] F. Galtarossa,[2] A. Goasduff,[4] F. Haas,[3] M. M. Mazzocco,[5] D. Montanari,[3] G. Montagnoli,[5] T. Mijatovic,[6] R. Sagaidak,[7] D. Santiago-Gonzalez,[8,1] F. Scarlassara,[5] E. E. Strano,[5] and S. Szilner[6]

[1]*Physics Division, Argonne National Laboratory, Argonne, Illinois 60439, USA*
[2]*INFN, Laboratori Nazionali di Legnaro, I-35020 Legnaro (Padova), Italy*
[3]*IPHC and University of Strasbourg, CNRS/IN2P3, 67037 Strasbourg Cedex 2, France*
[4]*CSNSM, CNRS/IN2P3 and University Paris-Sud, F-91405 Orsay Campus, France*
[5]*Dipartimento di Fisica e Astronomia, Universitá di Padova, and INFN, Sez. di Padova, IT-35131 Padova, Italy*
[6]*Ruder Boskovic Institute, HR-10002 Zagreb, Croatia*
[7]*Joint Institute for Nuclear Research, RU-141980 Dubna, Russian Federation*
[8]*Department of Physics and Astronomy, Louisiana State University, Baton Rouge, Louisiana 70803, USA*
(Received 13 January 2015; revised manuscript received 18 February 2015; published 3 April 2015)

Measurements of fusion excitation functions of ^{58}Ni + ^{124}Sn and ^{64}Ni + ^{124}Sn are extended towards lower energy to cross sections of 1 μb and are compared to detailed coupled-channels calculations. The calculations clearly show the importance of including transfer reactions in a coupled-channels treatment for such heavy systems. This result is different from the conclusion made in a previous article which claimed that the influence of transfer on fusion is not important for fusion reactions of Ni + Sn. In the energy region studied in this experiment no indication of fusion hindrance has been observed, which is consistent with a systematic study of this behavior.

DOI: 10.1103/PhysRevC.91.044602 PACS number(s): 25.70.Jj, 97.10.Cv, 97.10.Tk

I. INTRODUCTION

Heavy-ion-induced fusion reactions have been studied extensively during the last 30 years. Following the discovery of fusion enhancement at energies in the vicinity of the Coulomb barrier, coupled-channels (CC) calculations were used to explain this behavior and to extract the underlying barrier distributions. At lower energies a suppression of the fusion cross sections (fusion hindrance) was discovered about 10 years ago and explained through the saturation properties of nuclear matter. All of these phenomena have been summarized in several review articles [1–3].

While the coupling between fusion and inelastic channels is quite well understood in the CC calculations, the influence of transfer reactions is less clear. Its importance was first emphasized by Broglia *et al.* [4,5] and the first indications were observed experimentally in transfer measurements of ^{58}Ni + ^{58,64}Ni [6]. A CC model of this effect was developed early on [7] in an attempt to make a consistent description of the fusion, transfer, and elastic scattering data that had been obtained in the ^{58}Ni + ^{64}Ni collisions. This model was later applied [8] to analyze the neutron transfer data obtained in ^{58}Ni + ^{124}Sn collisions [9] to investigate their influence on fusion. Other earlier studies of the influence of transfer reactions on the fusion channel have been performed in the reactions of ^{33}S with a series of Zr isotopes [10,11].

Recently there has been an increase in the theoretical and experimental studies of the influence of transfer on fusion [12–23] because it was realized that, for a complete understanding of the reaction mechanism, transfer reactions have to be included [12,13]. Coupling to transfer reactions might also play a role in the study of fusion hindrance at extreme-sub-barrier energies by pushing the hindrance towards lower energies. In this article we discuss both effects for the Ni + Sn system.

Fusion between Ni and Sn isotopes has been studied for more than 30 years down to cross sections of about 0.1–1 mb [14,24–27]. While for the recent measurements with secondary beams of ^{132}Sn this cross section limit was caused by the beam intensities available at existing radioactive beam facilities, the interest in the earlier experiments with stable beams was in the relative contributions of fusion evaporation, fusion-fission, deep-inelastic scatterings, etc., to the capture process covering many isotopic combinations at energies close to the Coulomb barrier.

The influence of the coupling of transfer reactions on fusion in the system Ni + Sn was suggested [14] to be rather small, contrary to lighter systems. However, in a later publication [21] it was concluded that the fusion enhancement due to the transfer couplings is also present in heavier systems like Ni + Sn.

These different conclusions are to some extent caused by the fact that the fusion excitation functions in the Ni + Sn systems have only been measured down to the 0.1–1 mb region. To study the influence of transfer reactions in these heavier systems in more detail we have extended the fusion cross-section measurements for the ^{58}Ni + ^{124}Sn and ^{64}Ni + ^{124}Sn systems by 3–4 orders of magnitude into the μb region.

II. MEASUREMENT OF ^{58}Ni + ^{124}Sn AND ^{64}Ni + ^{124}Sn

The experiment was performed at the XTU Tandem accelerator of Laboratori Nazionali di Legnaro, Italy, using

*jiang@phy.anl.gov

doubly stripped beams of ^{58,64}Ni. The charge states of ^{58,64}Ni ions were 11^+ and 18^+ (or 17^+) after the first and second strippers, respectively. ^{58,64}Ni beams of 1–3 pnA bombarded a ^{124}Sn target with a thickness of 50 μg/cm^2, evaporated on a 20 μg/cm^2 carbon backing. The isotopic abundance of the ^{124}Sn target was 96.6%. The evaporation residues were detected with the Legnaro electrostatic separator in its upgraded configuration [28]. The detector system consisted of two micro-channel plate detectors, one ionization chamber, and a silicon surface-barrier detector. Four Si detectors placed around the target at 22.5° served as monitors. Pure Rutherford scattering cross sections were used to get the absolute cross sections for the evaporation residues. Details of the experimental setup and the analysis have been described previously in Refs. [28–31].

In the experiments two angular distributions in the range $\theta_{\rm lab} = -4°$ to 4° were measured at $E_{\rm lab} = 246.1$ and 234.0 MeV for the system ^{64}Ni + ^{124}Sn. These angular distributions can be well reproduced by two Gaussian components. For energies above $E_{\rm lab} \geqslant 229$ MeV the evaporation residues were detected at 1° and at 2°, while at the five lowest energies, only measurements at 1° were performed. In the experiment of ^{58}Ni + ^{124}Sn, only measurements at $\theta = 1°$ were taken. PACE [32] calculations showed that the angular distribution does not change much with energy nor with system in the Ni + Sn case.

At the low energies studied in these experiments, contributions from fusion-fission to fusion are usually small. At high energies, however, especially for the system ^{58}Ni + ^{124}Sn, this contribution can be comparable to the cross sections observed for evaporation residue production. Fusion-fission cross sections have been measured by Lesko *et al.* [25] for both systems and later by Wolfs *et al.* [26] for ^{58}Ni + ^{124}Sn. These fusion-fission cross sections are shown in Figs. 1 and 2 for ^{58}Ni + ^{124}Sn and ^{64}Ni + ^{124}Sn with open symbols. The fusion-fission cross sections from the earlier measurements were averaged and the interpolated values have been added to our measured evaporation residue cross sections to obtain the total fusion cross sections (black solid circles) in Figs. 1 and 2. At the low energies of our measurement the influence from fusion-fission reactions is small as can be seen from these two figures.

III. THE INFLUENCE FROM TRANSFER REACTIONS

The influence of inelastic and transfer reactions on the fusion channel is usually described by CC calculations. For heavier systems, however, these calculations become rather complex because more and more channels need to be included. For that reason, in a recent systematic study, the Wong formula was used to explore the contributions from transfer reactions to fusion [21]. The Wong formula, an analytic one [33], gives a good description of the fusion cross section in the region of 1000 to 1 mb (sometimes down to 0.1 mb) with only three parameters:

$$\sigma = \left(R_C^2/2E\right)\hbar\omega \ln\{1 + \exp[(2\pi/\hbar\omega)(E - V_C)]\}, \quad (1)$$

where R_C, V_C, and $\hbar\omega$ correspond to the radius, the height, and the curvature of the fusion barrier, respectively. It is well known that large $\hbar\omega$ values correspond to thin barriers, which are signatures of a strong fusion enhancement.

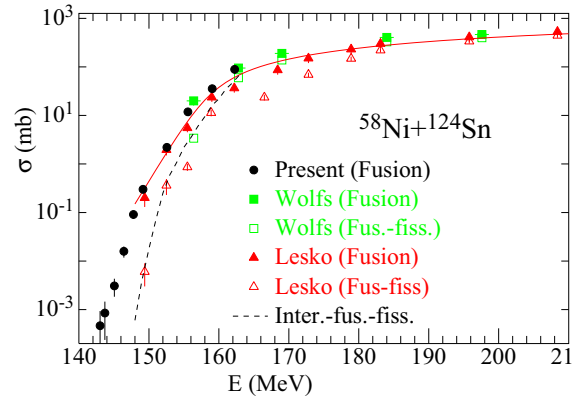

FIG. 1. (Color online) Cross sections of excitation functions for the system ^{58}Ni + ^{124}Sn plotted as functions of the c.m. energy. Black circles: Fusion cross sections measured in this experiment. Red triangles and red open triangles: Cross sections of fusion and fusion-fission reactions from Lesko *et al.* [25]. Green squares and green open squares: Cross sections of fusion and fusion-fission reactions from Wolfs *et al.* [26]. The red solid line is a fit with the Wong formula to fusion data with cross sections larger than 0.1 mb. The black dashed line represents the average fusion-fission cross sections used to obtain the total capture cross sections.

The results from least-squares fits with the Wong formula to the fusion reactions of ^{58,64}Ni + ^{124}Sn are shown by the solid lines in Figs. 1 and 2, respectively, and the resulting fit parameters are summarized in Table I together with those for the two other Ni + Sn systems, ^{58}Ni + ^{132}Sn and ^{64}Ni + ^{132}Sn. For comparison, fits for Ni + ^{124}Sn without using the present data are also included in Table I. In this case the uncertainty of $\hbar\omega$ from a fit to the data of Lesko *et al.* [25] for ^{64}Ni + ^{124}Sn is

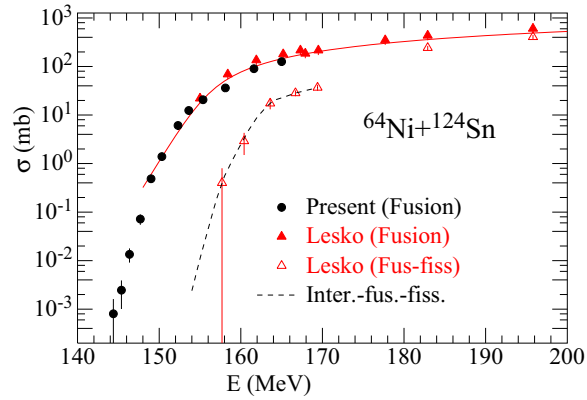

FIG. 2. (Color online) Cross sections of excitation functions for the system ^{64}Ni + ^{124}Sn plotted as functions of the c.m. energy. Black circles: Fusion cross sections measured in this experiment. Red triangles and red open triangles: Cross sections of fusion and fusion-fission reactions from Lesko *et al.* [25]. The red solid line is a fit with the Wong formula to fusion data with cross sections larger than 0.1 mb. The black dashed line represents the average fusion-fission cross sections used to obtain the total capture cross sections.

TABLE I. Comparison of the parameters $\hbar\omega$ and V_C obtained from fits with the Wong formula for the fusion reactions shown in Fig. 3 of Ni + Sn.

System	$\hbar\omega$ (MeV)	V_C (MeV)	Reference
^{58}Ni + ^{132}Sn	16.3 ± 1.0	159.2	Kohley *et al.* [14]
^{58}Ni + ^{124}Sn	11.4 ± 0.5	157.2	Lesko *et al.* [25] + Wolfs [26] + present
	12.2 ± 0.9	158.2	Lesko *et al.* [25] + Wolfs [26]
^{64}Ni + ^{132}Sn	11.1 ± 0.6	154.2	Liang *et al.* [27]
^{64}Ni + ^{124}Sn	9.8 ± 0.6	154.8	Lesko *et al.* [25] + present
	8.7 ± 7.5	154.8	Lesko *et al.* [25]

large (because of the limited range of cross sections) and was therefore not included in the discussion of Ref. [21].

Figure 3 is is an updated version of Figs. 3(c) and 3(d) from Ref. [21] including the new data for ^{64}Ni + ^{124}Sn (blue triangles) and ^{58}Ni + ^{124}Sn (black circles). As can be seen the excitation function of ^{64}Ni + ^{124}Sn has the steepest slope at low energies, corresponding to the smallest value of $\hbar\omega$, which correlates with the most negative Q values, and the smallest cross sections for neutron-transfer reactions. The fusion cross sections of ^{58}Ni + ^{124}Sn are smaller than the ones for ^{64}Ni + ^{124}Sn at higher energies but dominate at low energies as can be seen in this plot of σ vs $E - V_C$, providing evidence of the stronger couplings from transfer reactions in ^{58}Ni + ^{124}Sn when compared to those in ^{64}Ni + ^{124}Sn. The $\hbar\omega$ values also correlate well with the average Q value for neutron-transfer reactions shown in the insert of Fig. 3, with positive Q values corresponding to large values of $\hbar\omega$, i.e., thin barriers. The present experiments confirm the conclusions made in Ref. [21] that heavier systems such as Ni + Sn show the same correlation between the curvature $\hbar\omega$ of the fusion barrier and the Q value of the transfer reactions, which is a sign of a strong fusion enhancement.

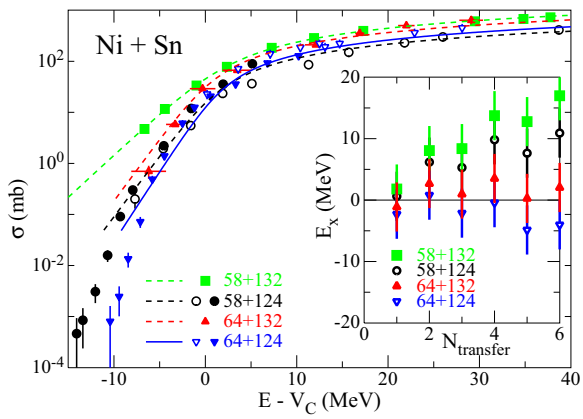

FIG. 3. (Color online) Fusion excitation functions for various Ni + Sn systems plotted as functions of $E - V_C$ where E is the c.m. energy and V_C is the Coulomb barrier taken from Table I. The curves are fits to the Wong formula. Insert: Average excitation energies of neutron pickup reactions calculated from the Q-value systematics for the same systems. Except for the systems ^{58,64}Ni + ^{124}Sn the cross sections are identical to the ones shown in Figs. 3(c) and 3(d) of Ref. [21].

IV. HINDRANCE IN HEAVY SYSTEMS

Hindrance of heavy-ion fusion at deep-sub-barrier energies was discovered about 10 years ago [34]. If the Q value for fusion is negative, as is the case for most of the medium and heavy systems, the fusion cross section has to reach zero at $E = -Q$. As a result the S factor, $S(E) = E\sigma(E)\exp(2\pi\eta)$, has to develop a maximum at deep-sub-barrier energies, E_s, and the logarithmic derivative, $L(E) = d[ln(E\sigma)]/dE$, has to cross the constant S-factor function, $L_{cs}(E) = \pi\eta/E$. Whether an S-factor maximum occurs also for fusion reactions with positive Q values, which is of interest to nuclear astrophysics, has been the topic of many reaction studies [3,35,36]. So far no clear indication of an S-factor maximum has been observed for these reactions with positive Q values. For heavier systems, one can find many examples of the hindrance phenomenon in the literature, ranging from ^{28}Si + ^{64}Ni [37] to ^{90}Zr + ^{90,92}Zr [38], which have been discussed in Refs. [3,39–41]. There it was derived that the energy E_s at which the maximum should occur follows the expression

$$E_s^{\mathrm{ref}} = (0.212\zeta)^{2/3}\ \ (\mathrm{MeV}), \qquad (2)$$

where ζ is a system-specific parameter given by $\zeta = Z_1 Z_2 \sqrt{A_1 A_2/(A_1 + A_2)}$.

This empirical expression is valid for negative-Q-value systems involving closed-shell nuclei in both projectiles and targets. For nuclei away from closed shells the energy of the maximum is shifted to energies that are lower than the prediction of Eq. (2) by 5–10 MeV. A plot of the experimentally determined maxima E_s vs ζ for several systems is shown in Fig. 4(a) [28,34,37,38,42–45]. For these systems the cross sections at these low energies are dominated by fusion-evaporation reactions. The solid circles in Fig. 4 involve systems with closed-shell nuclei while the stars are for open-shell nuclei. The dot-dashed line in Fig. 4(a) is the prediction of Eq. (2). The cross sections σ_s at the energy of the S-factor maximum show variations much larger than those observed for E_s. The two lines in Fig. 4(b) give the extreme values with neutron-deficient, closed-shell nuclei concentrating towards the upper solid line, while neutron-rich, open-shell nuclei (e.g., ^{64}Ni + ^{100}Mo) show cross sections closer to the lower dashed line.

The fusion Q values of the ^{58}Ni + ^{124}Sn and ^{64}Ni + ^{124}Sn systems are −112.3 and −117.5 MeV, respectively, and the ζ values are around 9000. Since the ^{58,64}Ni + ^{124}Sn systems are similar to the ^{64}Ni + ^{100}Mo system, based on the systematics

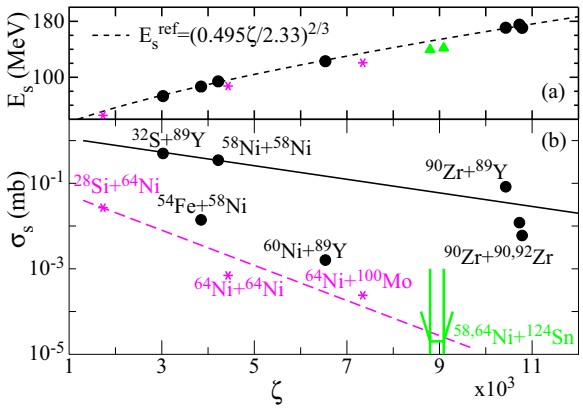

FIG. 4. (Color online) (a) Plot of the energy E_s, where a maximum of the S factor is observed versus ζ [$=Z_1Z_2\sqrt{A_1A_2/(A_1+A_2)}$]. The dot-dashed line is from Eq. (2). (b) Plot of the fusion cross sections σ_s measured at E_s as a function of ζ for the same systems shown in Fig. 4(a). The two lines give the range of σ_s. Neutron-deficient (closed-shell) systems are concentrated towards larger σ_s values while neutron-rich systems have smaller values of σ_s. The green symbols are the values of E_s and σ_s expected for the ^{58,64}Ni + ^{124}Sn systems. See text for details.

shown in Fig. 4, the maxima of the S factor are expected to occur at energies lower than 140 MeV, with σ_s values in the range around 1–10 nb.

From the experimental data in Figs. 1 and 2 one can see that these energy and cross-section limits have not been reached in the present experiment and, thus, no maximum of the S factor could be expected. In fact, from our results of these two systems, experimental $S(E)$ factors are increasing steadily until the lowest energies are reached. To see the hindrance behavior for these two systems an improvement in the measurements by a factor of ∼100 is needed.

V. COUPLED-CHANNELS CALCULATIONS

Coupled-channels calculations published previously [8] have given good descriptions of fusion and transfer reactions for the system ^{58}Ni + ^{124}Sn around the barrier using the cross sections from Refs. [9,25]. We have performed similar CC calculations but covering also the low-energy region for the ^{58}Ni + ^{124}Sn and ^{64}Ni + ^{124}Sn systems studied in this work. Because, as discussed in Sec. IV, no indication of fusion hindrance has been observed, a standard Woods-Saxon potential was used for the ion-ion interactions in the present calculations.

The parameters for inelastic excitations are listed in Table II. The values for ^{64}Ni are the same as the ones used to analyze the fusion of ^{64}Ni + ^{64}Ni in Ref. [44], and the parameters for ^{58}Ni and ^{124}Sn used are the same as in the previous CC analyses [8].

The spectroscopic factors for the strongest one-neutron pickup channels to ^{65}Ni and ^{59}Ni, leading to ^{123}Sn, are listed in Table III. For the ^{58}Ni + ^{124}Sn system, the $1n$ and $2n$ transfer strengths are calibrated to reproduce the $1n$, $2n$, and $3n$ transfer data [9]. The best fit to the transfer data requires a rescaling of the $1n$ transfer spectroscopic factors of Ref. [46] by a factor of $S_c = 0.85$ and of the $2n$ strength by a factor of $\alpha_{2n} = 0.04$ fm.

TABLE II. Low-lying states in ^{58,64}Ni and ^{124}Sn. The $B(E\lambda)$ values for ^{58}Ni and ^{124}Sn are the same as those used in Ref. [8]. The $B(E\lambda)$ values for ^{64}Ni are the same as those used in the analyses for fusion of ^{64}Ni + ^{64}Ni [44].

Nucleus	λ^π	E_{ex} (MeV)	$B(E\lambda)$(W.u.)	β_λ^C	σ_λ^C	σ_λ^N
^{58}Ni	2^+	1.454	10.2	0.183	0.24	0.28
	3^-	4.475	13.3	0.204	0.27	0.27
^{64}Ni	2^+	1.346	8.6	0.165	0.223	0.25
	3^-	3.560	12.0	0.193	0.261	0.27
^{124}Sn	2^+	1.132	9.0	0.095	0.16	0.16
	3^-	2.603	11.9	0.108	0.18	0.18

Similar calculations are performed for the system ^{64}Ni + ^{124}Sn using the same pair-transfer coupling strength, 0.04 fm, as used in Ref. [8].

The parameters of the Woods-Saxon potentials and the resulting barrier heights, radii etc., are summarized in Table IV. In the calculations, we found that a radius shift by $\Delta R = 0.25$ or 0.15 fm had to be added to the fusion radius of the reactions ^{58}Ni + ^{124}Sn or ^{64}Ni + ^{124}Sn, respectively, to give a good reproduction of the experimental data at low energies.

A comparison between the experimental data and the CC calculations for the systems ^{58}Ni + ^{124}Sn and ^{64}Ni + ^{124}Sn covering the whole energy range is given in Figs. 5 and 6. The no-coupling calculations are represented by the dot-dashed curves. The inclusion of transfer channels and inelastic scattering in the CC calculations is shown by the dotted and dashed lines, respectively, while the full calculations are represented by the solid lines. At energies above the barrier all calculations agree with each other. For the system ^{58}Ni + ^{124}Sn, where the cross sections for fusion-evaporation, fusion-fission, and deep-inelastic scattering have all been measured [26], the calculations are in good agreement with

TABLE III. Spectroscopic factors for one-neutron pickup by ^{58}Ni and ^{64}Ni and for one-neutron stripping by ^{124}Sn taken from Refs. [8,46], respectively. The ground-state Q values for one-neutron transfer are 0.508 and −0.239 MeV for the ^{58}Ni- and ^{64}Ni-induced reactions, respectively. The corresponding two-neutron transfer Q values are 5.949 and 0.614 MeV.

Nucleus	State	E_{ex} (MeV)	S factor
^{59}Ni	$p_{3/2}$	0	0.59
	$f_{5/2}$	0.339	0.71
	$p_{1/2}$	0.465	0.52
	$p_{3/2}$	0.878	0.10
^{65}Ni	$f_{5/2}$	0	0.218
	$p_{1/2}$	0.063	0.399
	$p_{3/2}$	0.310	0.022
	$p_{3/2}$	0.692	0.093
	$g_{9/2}$	1.017	0.738
^{123}Sn	$h_{11/2}$	0	4.50
	$d_{3/2}$	0.020	3.00
	$s_{1/2}$	0.139	1.90
	$d_{5/2}$	0.325	6.00

TABLE IV. Parameters of the Woods-Saxon potentials used in the CC calculations and the resulting values of the potential pockets and the associated radii.

System	DR (fm)	V (MeV)	R (fm)	a (fm)	V_C (MeV)	V_{pocket} (MeV)
^{58}Ni + ^{124}Sn	0.15	−84.35	10.599	0.687	158.37	141.42
^{58}Ni + ^{124}Sn	0.25	−84.35	10.699	0.687	156.95	139.32
^{64}Ni + ^{124}Sn	0.15	−86.25	10.754	0.690	155.88	136.74

the experimental capture data. At low energies, where deep-inelastic and fusion-fission contributions should be small, the solid lines representing the full CC calculations are again in good agreement with the data.

At energies in the vicinity of the barrier the CC calculations overpredict the fusion cross sections and one needs to include the yield from the deep-inelastic channel to achieve a reasonable agreement. Unfortunately these cross sections have so far been measured only for the ^{58}Ni + ^{124}Sn system and only at relatively high energies.

To study the influence of multiphonon excitations and transfer channels in the CC calculations in more detail, the low-energy parts of various calculations for the systems ^{58}Ni + ^{124}Sn and ^{64}Ni + ^{124}Sn are shown in Figs. 7 and 8 in an expanded scale in comparison with the experimental data. As in Figs. 5 and 6 the dot-dashed curve is the no-coupling calculation. The effect of including inelastic-scattering channels in the CC calculations is shown by the dashed lines. Including one- or two-phonon excitation results in 5 channels or 15 channels, as shown by the dashed black and light-blue lines, respectively. The latter calculation includes all one- and two-phonon states as well as mutual excitations of the low-lying 2^+ and 3^- states in the projectile and/or the target. In a three-phonon calculation, the three mutual one-phonon excitations and the mutual excitations of one- and two-phonon states are included but the three-phonon excitations of the same mode are excluded, resulting in 31 channels (see the red dashed lines, ch31).

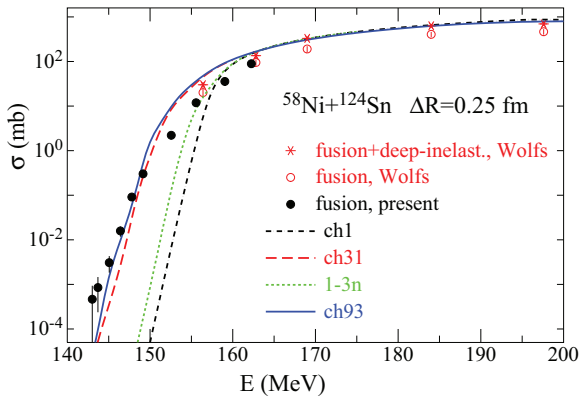

FIG. 5. (Color) Coupled-channels calculations for the fusion reaction ^{58}Ni + ^{124}Sn as a function of the c.m. energy, covering the full energy range.

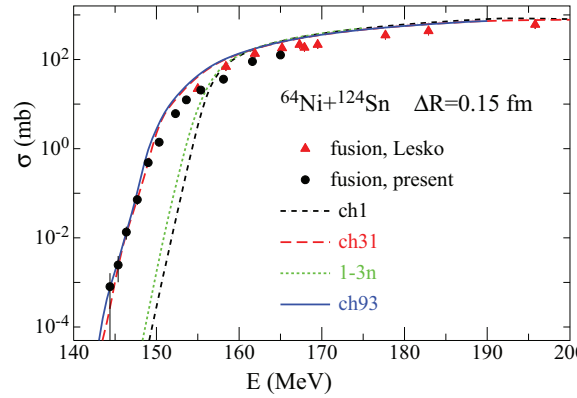

FIG. 6. (Color) Coupled-channels calculations for the fusion reaction ^{64}Ni + ^{124}Sn as a function of the c.m. energy, covering the full energy range.

The lines labeled 1–2n and 1–3n indicate calculations including only the coupling of one- and two- (1–2n) or one-, two-, and three-neutron transfer (1–3n), as shown by the magenta and green dotted lines, respectively. It is clear that the inclusion of more neutron-transfer reactions will not lead to further fusion enhancements.

Including the couplings of both inelastic (one-, two-, and three-phonon) and transfer (one and two neutron) reactions gives a total of 93 channels, which is represented by the blue line (ch93).

A comparison of Figs. 7 and 8 exhibits several interesting features. (i) As shown by the dashed lines the largest enhancement of the fusion cross sections is caused by inelastic excitations. There the enhancement of the fusion cross section converges with the inclusion of three-phonon excitations. (ii) As expected from the optimum Q-value systematics (see, e.g., the insert in Fig. 3), the system ^{58}Ni + ^{124}Sn exhibits a larger influence from transfer reactions when compared to the system ^{64}Ni + ^{124}Sn. This can be recognized from a comparison of the differences between no-coupling and the 1–2n (and 1–3n) calculations. From the calculations with 31 and 93 channels one can see that the effects of transfer reactions are more pronounced when the energy decreases

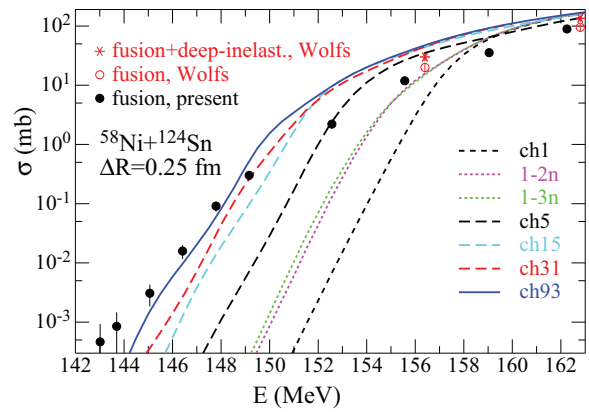

FIG. 7. (Color) Coupled-channels calculations for the fusion reaction ^{58}Ni + ^{124}Sn in the sub-barrier energy region.

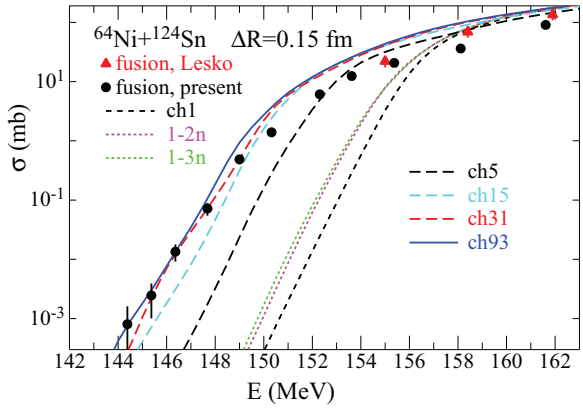

FIG. 8. (Color) Coupled-channels calculations for the fusion reaction ^{64}Ni + ^{124}Sn in the sub-barrier energy region.

into the cross-section range below 1 mb (a similar behavior has been seen in Ref. [20]). It should be mentioned that for the system ^{64}Ni + ^{124}Sn the contribution from transfer is weak due to the small transfer Q values but not negligible. (iii) Both systems, ^{58}Ni + ^{124}Sn as well as ^{64}Ni + ^{124}Sn, show a reduction of the experimental cross sections around 151 MeV compared to the CC calculations. The reason for this behaviour is not understood; but it may be partly due to the deep-inelastic scattering.

From the Q values for neutron-transfer reactions (see Fig. 3) one would expect that the ^{58}Ni + ^{132}Sn system should exhibit the largest influence of transfer reactions. However, as mentioned above this influence shows up mainly in the cross section region below 1 mb, where no fusion data have been measured so far.

VI. SUMMARY

Measurements of fusion excitation functions of the systems ^{58,64}Ni + ^{124}Sn have been extended to the ∼1 μb range. Detailed CC calculations have been performed studying the reaction mechanism of ^{58}Ni + ^{124}Sn and ^{64}Ni + ^{124}Sn over a large energy range. The calculations are in reasonable agreement with the new measurements, indicating that transfer reactions play the same critical role in heavy systems as seen previously for lighter systems.

No indication of an S-factor maximum has been observed in the new data. This is in agreement with the systematics observed from other systems, which predicts an S-factor maximum at energies below 140 MeV. Measurements at these energies require an improvement of the detector techniques by a factor of 100.

ACKNOWLEDGMENTS

We want to thank the staff of the XTU Tandem for providing the excellent high-energy ^{58}Ni and ^{64}Ni beams. This work was supported by the US Department of Energy, Office of Science, Office of Nuclear Physics, under Contract No. DE-AC02-06CH11357, and the European Union Seventh Framework Programme FP7/2007-2013 under Grant No. 262010-ENSAR. A.G. was partially supported by the P210 Excellence Laboratory.

[1] M. D. Dasgupta, D. J. Hinde, N. Rowley, and A. M. Stefanini, Annu. Rev. Nucl. Part. Sci. **48**, 401 (1998).
[2] A. B. Balantekin and N. Takigawa, Rev. Mod. Phys. **70**, 77 (1998).
[3] B. B. Back, H. Esbensen, C. L. Jiang, and K. E. Rehm, Rev. Mod. Phys. **86**, 317 (2014).
[4] R. A. Broglia, C. H. Dasso, S. Landowne, and A. Winther, Phys. Rev. C **27**, 2433(R) (1983).
[5] R. A. Broglia, C. H. Dasso, S. Landowne, and G. Pollarolo, Phys. Lett. B **133**, 34 (1983).
[6] K. E. Rehm, F. L. H. Wolfs, A. M. van den Berg, and W. Henning, Phys. Rev. Lett. **55**, 280 (1985).
[7] H. Esbensen and S. Landowne, Nucl. Phys. A **492**, 473 (1989).
[8] H. Esbensen, C. L. Jiang, and K. E. Rehm, Phys. Rev. C **57**, 2401 (1998).
[9] C. L. Jiang *et al.*, Phys. Rev. C **57**, 2393 (1998).
[10] L. Corradi *et al.*, Z. Phys. A **334**, 55 (1990).
[11] L. Corradi *et al.*, Z. Phys. A **346**, 217 (1993).
[12] G. Pollarolo and A. Winther, Phys. Rev. C **62**, 054611 (2000).
[13] G. Pollarolo, Phys. Rev. Lett. **100**, 252701 (2008).
[14] Z. Kohley *et al.*, Phys. Rev. Lett. **107**, 202701 (2011).
[15] J. J. Kolata *et al.*, Phys. Rev. C **85**, 054603 (2012).
[16] V. V. Sargsyan, G. G. Adamian, N. V. Antonenko, W. Scheid, and H. Q. Zhang, Phys. Rev. C **85**, 024616 (2012).
[17] V. V. Sargsyan, G. G. Adamian, N. V. Antonenko, W. Scheid, and H. Q. Zhang, Phys. Rev. C **86**, 034614 (2012).
[18] H. M. Jia *et al.*, Phys. Rev. C **86**, 044621 (2012).
[19] V. V. Sargsyan, G. Scamps, G. G. Adamian, N. V. Antonenko, and D. Lacroix, Phys. Rev. C **88**, 064601 (2013).
[20] A. M. Stefanini *et al.*, Phys. Lett. B **728**, 639 (2014).
[21] C. L. Jiang, K. E. Rehm, B. B. Back, H. Esbensen, R. V. F. Janssens, A. M. Stefanini, and G. Montagnoli, Phys. Rev. C **89**, 051603(R) (2014).
[22] G. L. Zhang, X. X. Liu, and C. J. Lin, Phys. Rev. C **89**, 054602 (2014).
[23] D. Bourgin *et al.*, Phys. Rev. C **90**, 044610 (2014).
[24] W. S. Freeman, H. Ernst, D. F. Geesaman, W. Henning, T. J. Humanic, W. Kuhn, G. Rosner, J. P. Schiffer, B. Zeidman, and F. W. Prosser, Phys. Rev. Lett. **50**, 1563 (1983).
[25] K. T Lesko *et al.*, Phys. Rev. Lett. **55**, 803 (1985); Phys. Rev. C **34**, 2155 (1986).
[26] F. L. H. Wolfs, W. Henning, K. E. Rehm, and J. P. Schiffer, Phys. Lett. B **196**, 113 (1987); F. L. H. Wolfs, Phys. Rev. C **36**, 1379 (1987).
[27] J. F. Liang, D. Shapira, C. J. Gross, R. L. Varner, J. R. Beene, P. E. Mueller, and D. W. Stracener, Phys. Rev. C **78**, 047601 (2008).
[28] A. M. Stefanini *et al.*, Phys. Rev. C **82**, 014614 (2010).
[29] A. M. Stefanini *et al.*, Phys. Rev. C **78**, 044607 (2008).

[30] A. M. Stefanini *et al.*, Phys. Lett. B **679**, 95 (2009).
[31] A. M. Stefanini *et al.*, Phys. Rev. C **81**, 037601 (2010).
[32] A. Gavron, Phys. Rev. C **21**, 230 (1980).
[33] C. Y. Wong, Phys. Rev. Lett. **31**, 766 (1973).
[34] C. L. Jiang *et al.*, Phys. Rev. Lett. **89**, 052701 (2002).
[35] C. L. Jiang *et al.*, Phys. Rev. Lett. **113**, 022701 (2014).
[36] G. Montagnoli *et al.*, Phys. Rev. C **90**, 044608 (2014).
[37] C. L. Jiang *et al.*, Phys. Lett. B **640**, 18 (2006).
[38] J. G. Keller, K. H. Schmidt, H. Stelzer, W. Reisdorf, Y. K. Agarwal, F. P. Hessberger, G. Munzenberg, H. G. Clerc, and C. C. Sahm, Phys. Rev. C **29**, 1569 (1984); Nucl. Phys. A **452**, 173 (1996).
[39] C. L. Jiang, H. Esbensen, B. B. Back, R. V. F. Janssens, and K. E. Rehm, Phys. Rev. C **69**, 014604 (2004).
[40] C. L. Jiang, B. B. Back, H. Esbensen, R. V. F. Janssens, and K. E. Rehm, Phys. Rev. C **73**, 014613 (2006).
[41] C. L. Jiang, B. B. Back, R. V. F. Janssens, and K. E. Rehm, Phys. Rev. C **75**, 057604 (2007).
[42] A. Mukherjee *et al.*, Phys. Rev. C **66**, 034607 (2002).
[43] M. Beckerman *et al.*, Phys. Rev. C **23**, 1581 (1981).
[44] C. L. Jiang *et al.*, Phys. Rev. Lett. **93**, 012701 (2004).
[45] C. L. Jiang *et al.*, Phys. Rev. C **71**, 044613 (2005).
[46] J. Lee, M. B. Tsang, W. G. Lynch, M. Horoi, and S. C. Su, Phys. Rev. C **79**, 054611 (2009).